CONCEPT FOR THE ANTIPROTON PRODUCTION TARGET AT FAIR

K. Knie, A. Dolinskii, B. Franzke, V. Gostishchev, M. Steck, GSI, Darmstadt, Germany
P. Sievers, CERN, Geneva, Switzerland

Abstract

This report summarizes the status of the antiproton (pbar) production area at the future FAIR (Facility for Antiproton and Ion Research) complex at GSI, Darmstadt [1]. This area is composed of the pbar production target, a magnetic horn for the collection of the pbars, and the pbar separator between target and Collector Ring (CR).

The emphasis is on the optimization of the accumulation rate of antiprotons to maximize the expected peak and average luminosity for the experiment.

As the doses in the target area will be very high, also radiation protection issues will be addressed.

INTRODUCTION

Antiprotons are generated in inelastic collisions of high energy protons with nucleons of a target nucleus at rest by the process p + A → pbar + X, where X represents all the other particles in any final quantum state allowed in the collision, i.e. the scattered projectile proton, the proton from the pbar-p pair, other hadron or lepton pairs ("shower"), and the residue of the target nucleus with the initial mass number A. Taking into account the kinetic energy of the center of mass (c.m.) of the interacting primary nucleons the process requires a minimum kinetic proton energy in the laboratory system above the pbar threshold of 6 $m_p c^2$ = 5.6 GeV, with m_p as the rest mass of the (anti)proton.

At the former Antiproton Accumulation Complex (AAC) at CERN [2], the antiproton production was done with 25 GeV protons from the proton synchrotron with cycle periods of 4.8 s and an intensity of 1.45×10^{13} primary protons per pulse (ppp). Due to the higher energy of the synchrotrons at Fermilab [3, 4] the antiproton production is performed with 120 GeV protons with about 8×10^{12} ppp and a cycle length of 2.2 s.

At FAIR a proton beam from the SIS100 synchrotron [5] with a kinetic energy of 29 GeV and a maximal intensity of 2.5×10^{13} ppp will be used for the pbar. Although the production yields increase with the proton energy, we favour a kinetic energy of 29 GeV instead of 90 GeV (which would be achievable with the planned SIS300) for several reasons:

i) For protons at 29 GeV the maximum overall yield is already achieved for an antiproton energy around 3 GeV, which corresponds to a moderate magnetic rigidity of 12.7 Tm. For a kinetic energy of 90 GeV the maximum yield is around 9 GeV/c, thus a succeeding beam transport system and storage rings with a much higher bending power of around 30 Tm would be required.

ii) The lower energy of the antiprotons allows a more efficient collection of the antiprotons, especially of those with larger angles to the beam axis.

iii) For an efficient cooling in the CR bunches with $t < 50$ ns are indispensable. A corresponding bunch compression system for the SIS300 would be very demanding and is not foreseen.

Every 10 seconds 2.5×10^{13} protons will be accelerated in the SIS100 to 29 GeV and compressed into a bunch of 50 ns. Antiprotons will be produced in collision of these protons with a metal target. Immediately behind the target, a pulsed magnetic horn will be placed to collect the antiprotons emerging from the target with energies around 3 GeV and within a cone of about 80 mrad.

The separation of the antiprotons from primary protons and other secondary particles will be provided the succeeding pbar separator, which transfers antiprotons to the collector ring CR [6]. In this line transverse and momentum collimation takes place. The antiprotons within the separator's acceptance ($\varepsilon_x = \varepsilon_y = 240\pi$ mm mrad, $\Delta p/p = \pm 3\%$), will be transferred to the CR with nearly 100 % transmission. The setup of the pbar production area is depicted in fig. 4.

PBAR COLLECTION

After their creation in the target, the antiproton and proton are not at rest in the c.m. system of the two interacting nucleons. Their angular distribution is isotropic in this frame. Hence, the antiproton velocity distribution in the laboratory system has its maximum near the c.m. velocity, and they have a wide angular distribution. Using the semi-empirical formula from Duperray [7], it can be calculated that for 29 GeV primary protons and 3 GeV antiprotons the production yield with respect to the angular distribution has its maximum at nearly 100 mrad, which demands a powerful first optical element in the transfer line which focuses the antiprotons to a small angular divergence. It is planned, to use a magnetic horn for this purpose. It produces a circular magnetic field, which is capable to bend antiprotons with angles θ up to 80 mrad parallel to the beam axis as shown in fig. 1. A magnetic horn similar to that one presently operated at CERN [8] will be used at FAIR. Like at CERN, it will be pulsed with a current of 400 kA.

The effect of the magnetic horn is shown in fig. 1. The blue dots correspond to a particle distribution in the x-x' plane right after the target. This initial distribution was obtained by means of the MARS code [9]. A momentum cut ($\Delta p/p = \pm 3\%$) has been applied already. The magnetic horn rotates this distribution by 90°, thus the majority of the particles are within the acceptance of the separator behind the horn.
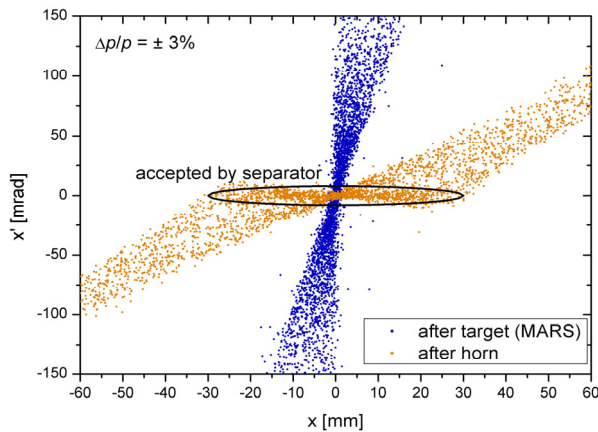
Figure 1: Phase space diagram of pbars after the target (blue dots) and the horn (orange dots).

PBAR YIELD FOR THE SYSTEM TARGET-HORN

Though our system is based on the former AAC concept at CERN, there are some differences. At FAIR the primary proton beam of 29 GeV is planned to be used instead of 25 GeV at AAC, the energy of the selected antiprotons will be 3 instead of 2.7 GeV. Also considering a somewhat higher acceptance of the separator (240 π mm mrad instead of 200 π mm mrad) one can expect an antiproton yield which is about 40 % higher than at AAC.

The production yield for pbars increases with the target thickness until the absorption of the protons and pbars in the target becomes dominant. Therefore, there is an optimum target length. Obviously, this length depends on the target's density. Because of a more point-like geometry, the collection efficiency is higher for a short target, thus high density materials like iridium (ρ = 22.56 g cm^{-3}) should be favored from this point of view.

On the other hand, all high density (i.e. high Z) materials have a low heat capacity. In addition, the cascade of secondaries cannot spread out as much as in materials with lower density. As a consequence, there will be a large temperature increase in high Z materials after an intense proton pulse as can bee seen in fig. 2. To avoid a melting of the target, relatively large beam diameters have to be chosen, which, however, results in reduced collection efficiencies. In addition, also the diameter of the target rod has to be increased, which results in an increased self-absorption in the target.

In summary, the highest yields (without melting the target with 2.5×10^{13} protons per pulse) can be expected for an about 11 cm long copper or nickel target. With about 2×10^{-5} pbars (in the ellipse in fig. 1) per primary proton this yield is more than 10 % higher than that of an 8 cm iridium target (see fig. 3). A more detailed description of these simulations is given in ref [10].
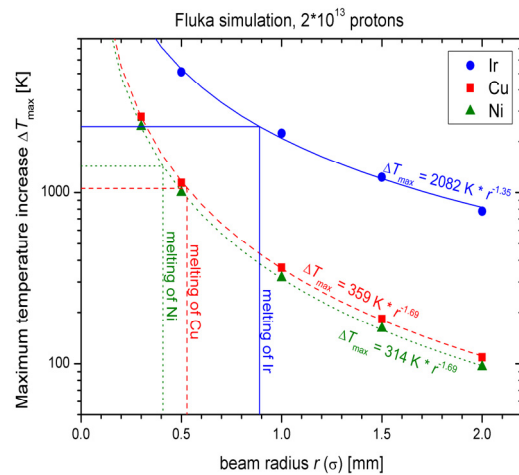

Figure 2: Maximum temperature increase after a pulse of 2×10^{13} primary protons versus the proton beam radius. The calculations were performed with FLUKA.
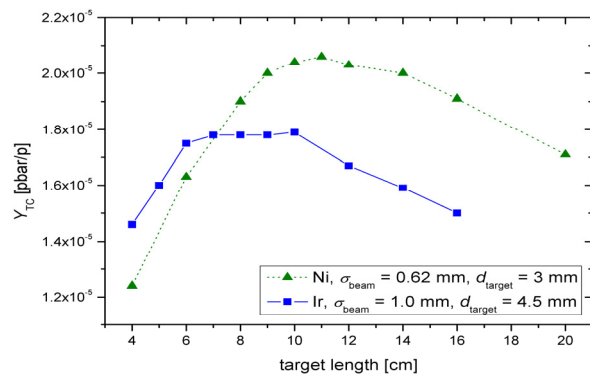

Figure 3: Comparison of antiproton yields after target and magnetic horn for different target materials and different sizes of the primary proton beam versus the target length. The target diameter is chosen for an optimum yield for the respective beam size.

CIVIL CONSTRUCTION AND RADIATION PROTECTION

In order to ensure that a sufficient radiation protection of the neighboring areas can be achieved, extensive simulations were performed with the Monte-Carlo particle transport code FLUKA [11]. A very detailed geometry file was needed as input to obtain reliable results. Magnetic fields in the magnetic horn and all quadrupole and dipole magnets were taken into account.

Due to the high energies and the long ranges of the primary and secondary particles a large region of 50 × 30 × 200 m³ was used in the FLUKA calculations (see fig. 4 and 5).

The target and magnetic horn are located in an iron shielding with 1.6 m thickness on the downstream side and 1.0 m thickness on all other sides. Between the buildings mainly concrete was used as shielding material.

According to the German Radiation Protection Ordinance areas with dose rates below 0.5 μSv/h (purple and white in fig. 5) are accessible without any restriction. This can be guaranteed for the neighboring experimental hall (building 50), the inner part of the CR hall (building 7) and for the upper levels of the pbar-target building (cannot be seen on fig. 5).
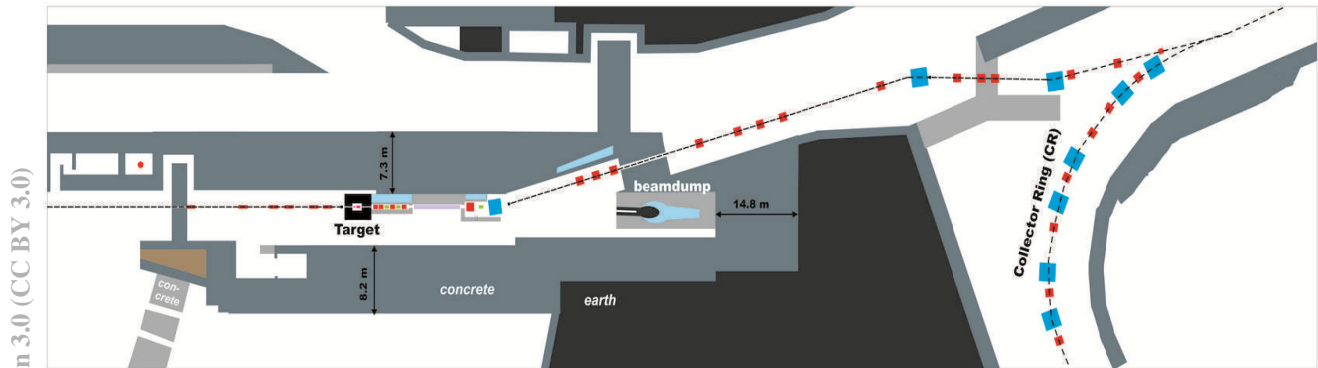

Figure 4: Schematic view of the pbar production area. The beam direction is from left to right. On the right side a part of the CR is shown.
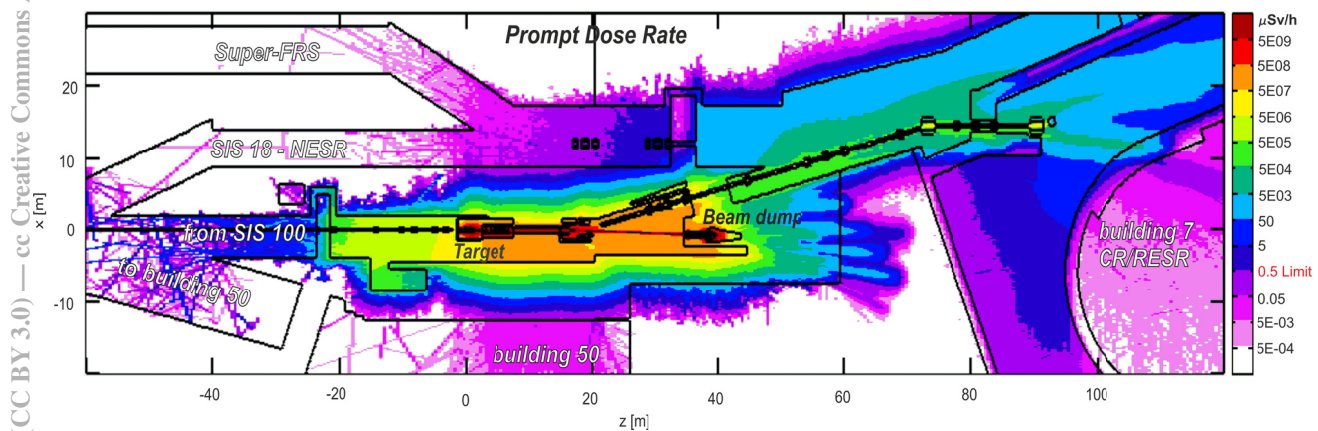

Figure 5: Equivalent dose rates during the production of pbars at maximum intensity.

REFERENCES

[1] An international accelerator facility for beams of ions and antiprotons, Conceptual Design Report, GSI-Darmstadt, 2001. www.gsi.de

[2] J.V. Allaby, CAS lectures, CERN/PS-AA/83-46, (1983) 63.

[3] D. McGinnis, Proceedings of the Particle Accelerator Conference, Knoxville, 2005, p. 484.

[4] R.J. Pasquinelli et. al., Proceeding of the Particle Accelerator Conference, Vancouver, 2009, TU6PFP075.

[5] P. Spiller and G. Franchetti, NIM A 561 (2006) 305.

[6] A. Dolinskii et al., NIM A 532 (2004) 483.

[7] R.P. Duperray et al., Phys. Rev. D 68 (2003) 094017.

[8] D. Boimond et al., CERN/PS 94-02 (AR) (1994).

[9] N.V. Mokhov, Fermilab-FN-628 (1995); O.E. Krivosheev, N.V. Mokhov, Proc. Monte Carlo 2000 Conf., p. 943, Lisbon, October 23-26, 2000. Fermilab-Conf-00/181 (2000); N.V. Mokhov, "Status of MARS Code", Fermilab-Conf-03/053 (2003); N.V. Mokhov et al., Fermilab-Conf-04/053 (2004); http://www-ap.fnal.gov/MARS/.

[10] A. Dolinskii et al., NIM A 629 (2011) 60.

[11] A. Fassò et al., CERN-2005-10 (2005), INFN/TC_05/11, SLAC-R-773; G. Battistoni et al., Proceedings of the Hadronic Shower Simulation Workshop 2006, Fermilab 6-8 September 2006, M. Albrow, R. Raja eds., AIP Conference Proceeding 896, 31-49, (2007).